Specular Reflection, Gloss, Roughness and Surface Heterogeneity of Biopolymer Coatings

T. A. TREZZA,[1]* J. M. KROCHTA[2]

[1] Frito Lay, Inc., 7701 Legacy Drive, Plano, Texas 75024, USA

[2] Department of Food Science and Technology, University of California, Davis, California 95616, USA

Received 24 January 2000; accepted 23 June 2000

ABSTRACT: The gloss values of biopolymer coatings were predicted by the Fresnel model from solid film refractive index measurements. Measured gloss properties of transparent coatings fit the model better than did those of wax- or lipid-dispersion coatings. Lipid content and particle size of dispersion coatings had a large influence on coating gloss. The effect of surface roughness on gloss was small compared with that of surface heterogeneity. Whey protein isolate and shellac coatings had higher gloss than hydroxypropyl methylcellulose coatings. © 2001 John Wiley & Sons, Inc. J Appl Polym Sci 79: 2221–2229, 2001

Key words: biopolymer coatings; specular gloss; roughness; optical properties; surface chemistry

INTRODUCTION

Gloss is an important quality factor of many food products.[1] Numerous studies have shown that the gloss of chocolate dramatically influences flavor judgment.[2] Foods such as apples, citrus fruits, vegetables, and confectionery products are coated with waxes and glazes to provide a high gloss.[3,4] However, the literature provides little data on the gloss properties of edible coatings. A greater understanding of these properties will allow food product formulators to optimize the gloss of a coated food product. Edible coatings made from whey proteins have the potential to improve the quality of foods, especially gloss. Whey protein isolate (WPI) coatings are excellent oxygen and aroma barriers, but only moderate moisture barriers.[5] To improve WPI coating moisture barriers, waxes can be added.[6,7] Lipids have been found to qualitatively reduce the shine of WPI coatings.[6] Also, Hagenmaier and Baker[8] found that lipids influenced the gloss of gelatin- and hydroxypropyl methylcellulose (HPMC)-candelilla wax-dispersion coatings. The gloss of paint coatings, with and without pigments, has been quantitatively determined from fundamental principles of optics.[9] The objectives of this study were the following: 1. predict the gloss of WPI and other biopolymer coatings from the Fresnel model, 2. measure the true gloss of these coatings as a function of lipid content, and 3. determine whether the Fresnel model could be used to accurately predict coating gloss.

Aspects of Gloss

Gloss relates to the ability or capacity of a surface to direct reflected light.[10,11] Gloss is not a single parameter, but a number of surface phenomena that constitute the light-reflecting properties of a

* Formerly with the Department of Food Science and Technology, University of California, Davis, CA.

Correspondence to: T. A. Trezza. (thomas.a.trezza@fritolay.com).

Journal of Applied Polymer Science, Vol. 79, 2221–2229 (2001)

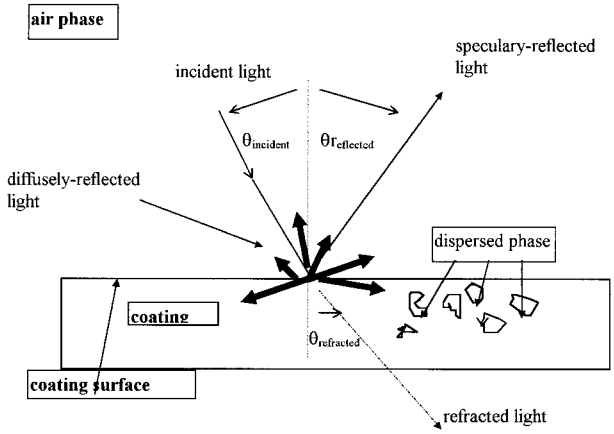

Figure 1 Schematic of light interacting with a surface.

surface.[12] The most well known type of gloss, which gives the perception of a "shiny" surface, is specular gloss.[13] Examples of other types of gloss are distinctness-of-image gloss, surface-uniformity gloss, and contrast gloss.[12,14] The effect of specular gloss is clearly seen with mirrors and polished metal surfaces.[9] Although specular gloss can be described mathematically and measured quantitatively, it cannot account for all of the light-reflecting properties of a surface. There is no single equation that can calculate all types of gloss, or a single instrument that can measure all types.[10] This report deals only with specular gloss.

THEORY

When a beam of light is incident upon a surface, some of the light is reflected and some of the light enters the object, where it is absorbed, refracted, or scattered (Fig. 1). Every surface reflects some light at an angle equal to the angle of incidence (specularly reflected), as well as some light in all other directions (diffusely reflected).[15] Specular reflectance is defined as the ratio of the intensity of the reflected beam to the intensity of the incident beam of light at a specific angle of incidence.[9,11] Specular reflectance is a function of refractive index of the surface (n), the extinction index (k), the angle of incidence of the beam of light (θ), and the nature of the reflecting light.[16] The quantities n and k are referred to as the optical constants of the material.[17,18]

Nonabsorbing Surfaces ($k = 0$)

For isotropic, homogeneous, optically smooth surfaces that do not show diffuse reflection and are essentially nonabsorbing, specular reflectance is governed only by the n, θ, and the polarization state of the incident light.[9,16] For optically smooth surfaces (e.g., a mirror), the coefficients of reflectance r_s and r_p can be calculated from Fresnel's theory:

$$r_s = \frac{n_1 \cos\,\theta_1 - n_2 \cos\,\theta_2}{n_1 \cos\,\theta_1 + n_2 \cos\,\theta_2} \tag{1}$$

$$r_p = -\frac{n_2 \cos\,\theta_1 - n_1 \cos\,\theta_2}{n_2 \cos\,\theta_1 + n_1 \cos\,\theta_2} \tag{2}$$

Here r_s and r_p are the coefficients of reflection for light polarized parallel and perpendicular to the incident light plane, respectively. The parameters n_1, n_2, θ_1, and θ_2 are the refractive index of medium 1 (typically air), the refractive index of medium 2 (liquid, solid or vapor), the angle of incidence of light, and the angle of refraction, respectively.[16,19] The specular reflectances R_s and R_p for parallel and perpendicular polarized light can then be calculated as[16,19]:

$$R_s = r_s^2 \tag{3}$$

$$R_p = r_p^2 \tag{4}$$

By applying Snell's law of refraction ($n_1 \sin\theta_1 = n_2 \sin\theta_2$), it is possible to relate the reflectance values to the angle of incidence of light and the refractive indices of the media through which the light is passing. For a surface where medium 1 is air ($n_1 \approx 1.000$), the following expressions for R_s and R_p result:

$$R_s = \left(\frac{\cos\,\theta_1 - (n^2 - \sin^2\theta_1)^{0.5}}{\cos\,\theta_1 + (n^2 - \sin^2\theta_1)^{0.5}}\right)^2 \tag{5}$$

$$R_p = \left(\frac{n^2 \cos\,\theta_1 - (n^2 - \sin^2\theta_1)^{0.5}}{n^2 \cos\,\theta_1 + (n^2 - \sin^2\theta_1)^{0.5}}\right)^2 \tag{6}$$

Typically, unpolarized light is used for gloss measurements.[16,20] For unpolarized light, the total reflectance (R) is calculated as the average of the parallel and perpendicularly polarized beams[9,16,20]:

$$R_{\text{unpolarized}} = \frac{1}{2}(R_p + R_s) \quad (7)$$

Last, gloss (G^θ) is calculated as the percentage of reflectance of the sample to that of a standard surface at an angle of incidence θ.

Absorbing Surfaces ($k \neq 0$)

Equations must be modified when the extinction index of the solid is not zero.[16,21] In these cases, the complex refractive index ($\tilde{N}$) must be substituted for the simple refractive index (n), where $\tilde{N} = n + ik$.[16,21] For absorbing media, Maxwell's equation for the propagation of a damped wave must be solved using the complex refractive index. The equations become large and cumbersome. Detailed derivations of the equations used for absorbing media can be found elsewhere.[17,22–24]

Physical Effects

Besides the absorption of light by the surface, the physical state of the surface can influence gloss. Rough or chemically heterogeneous surfaces can cause scattering of light, which reduces gloss.

Roughness

Surface roughness effects on gloss on polished metal surfaces have been well studied.[25] The Raleigh criteria[9,16,26]

$$h < \lambda/8 \cos \theta \quad (8)$$

can be used to determine when a surface is considered rough.[13,14] Here, h is the maximum defect height allowable for a surface to be considered optically smooth (not rough), and λ and θ are the wavelength and angle of incident light, respectively. A rough surface will have a large effect on the amount of light that is specularly reflected from that surface.[9]

To determine the roughness in practical systems, a model was developed that assumed a randomly rough surface on which the distribution of surface defect heights was normally distributed.[14] The roughness can then be determined from the reflectance of the sample from the following expression[9,14,25,27]:

$$R = R_0 \exp - ((4\pi\sigma \cos \theta)/\lambda)^2 \quad (9)$$

This expression is sometimes referred to as the Bennet-Porteus model.[9] Here R is the sample reflectance of a rough surface, R_o is the reflectance from an optically smooth surface of the same material, and σ is the root-mean-square roughness (nm). R_o, which is the same value as $R_{\text{unpolarized}}$ for the optically smooth surface, is typically calculated from eqs. (5), (6), and (7).[9] The common procedure for determining σ is to measure R at a number of angles, θ, then plot $\text{Ln}(R/R_o)$ against $(4\pi\cos\theta/\lambda)^2$. If a line results, the slope yields $-\sigma^2$. Because the model assumes that σ is normally distributed, the maximum defect height is 6σ.[28]

Heterogeneous Surfaces

Besides roughness, nonhomogeneous surfaces can reduce gloss. Chemical heterogeneity occurs when components are not uniformly distributed across a surface.[29] For example, a common cause of heterogeneity in paint films is pigment flocculation, leading to patches or clusters of pigments at the coating–air interface.[9] The surface is then left with a nonuniform distribution of pigment–polymer interfaces, capable of scattering light more effectively. It is important to understand that a heterogeneous surface is not necessarily rough. When a coating contains dispersed particles, the shape and size distributions of dispersed phases are also factors that influence gloss.[9]

MATERIALS AND METHODS

Coating Formulations

All coatings were made from liquid solutions or dispersions. Coating formulations were typical of those reported for use as coatings for foods and confectionery products.[30] Plasticizers were added at typical levels after correction of base coating-forming material for moisture content.

WPI

Ten percent (wt/wt) solutions of WPI (Food Grade; Bipro, Davisco Inc., LeSeur, MN) were prepared using magnetic stirring. Glycerol (GLY) (USP/FCC; Fisher Scientific, Fairlawn, NJ) was added as a plasticizer at a level of 2 parts WPI to 1 part GLY, on a dry solids basis. This solution was heated in a water bath at 90°C for 30 min to denature the protein, then quickly cooled (within 5 min) in a water-ice slush to 25°C. Finally, the solution was strained through two layers of

cheesecloth to remove gel particles that might have formed during heating. WPI coatings were formulated with and without Span 20 (sorbitan monolaurate; Sigma Chemical, St. Louis, MO). When added, final Span 20 concentrations were 0.36% on a dry solids basis.

Lipid dispersion coatings were produced by emulsifying carnauba wax (CW) (Food Grade; Strahl and Pitsch, West Babylon, NY) or anhydrous milk fat (AMF) (Level Valley Dairy, West Bend, WI) into the WPI-GLY solutions described above. For CW, a Microfluidizer homogenizer (HC-5000; Microfluidics International Corp., Newton, MA) was used to emulsify 40% wax (dry solids basis) in the WPI-GLY solution. The solution was heated and maintained at 90° C to ensure that CW remained liquid. Hot WPI-CW mixtures were passed through the homogenizer three times, using a head pressure of 5800–6100 psig for each pass. AMF dispersions containing 40% (dry solids basis) lipid in the WPI-GLY solutions were made with a Crepaco homogenizer (Crepaco Inc., Chicago, IL) using three passes at 8500 psig. Lower CW or AMF content coatings were created by diluting concentrated emulsions with stock WPI-GLY solution. It was assumed that the particles in the dry coatings were solid because the melting points of the CW and AMF used in this study were 83–86°C and 35–40°C, respectively.

Shellac

Dewaxed, bleached shellac (Food Grade, Type R-49; Mantrose-Haeuser Co., Attleboro, MA) was dissolved in 95% ethanol to form 29% (wt/wt) solutions. Propylene glycol (PG) (USP/FCC grade; Texaco Chemical Co., Houston, TX) was added at 1 part PG to 9 parts shellac, on a dry solids basis. Solutions were stirred until completely dissolved, then strained through two layers of cheesecloth.

The homogenizers used for WPI dispersions were not used for shellac because the equipment was not explosion proof. Shellac-CW dispersions were made by grinding a 47.6% (dry solids basis) dispersion of powdered CW (Food Grade; Strahl and Pitsch) in a media mill for 62 h. Wax particle size was monitored until it became a constant value. Lower wax-level dispersions were created by diluting the concentrated dispersion with CW-free shellac-ethanol solution.

Zein

Fourteen percent zein coating solutions were prepared by dissolving zein (FC 4000; Freeman Industries, Tuckahoe, NY) in 95% ethanol. PG (USP/FCC grade; Texaco Chemical Co.) was then added to a level of 1 part PG to 3 parts zein, on a dry solids basis. Final zein solutions contained 18% (wt/wt) of solids.

HPMC

Five percent (wt/wt) solutions of HPMC (Methocel E5 Premium; Dow Chemical Co., Midland, MI) were prepared according to the manufacturer's instructions. The process consisted of dispersing HPMC powder into 1/3 of the total required amount of water at 85°C, followed by gentle stirring until the powder was wetted and a consistent dispersion was obtained. The remaining 2/3 of water was then added, and the dispersion was mixed until it became a clear solution. The solution was then removed from the heat and mixed until it equilibrated to room temperature. Finally, GLY was added to a 5:1 (wt/wt) ratio of HPMC to GLY, on a dry solids basis.

Coating Casting and Drying

Liquid coating formulations were cast on 4″ × 7″ × 1/8″ thick sheets of matte black acrylic plastic (TAP Plastics, Sacramento, CA) using a Bird-type applicator (Paul Gardner Co., Pompano Beach, FL). Coatings were then dried at ambient conditions [23–25°C, 35–45% relative humidity (RH)] for 16 h. Dry coating thicknesses were 25 μm.

Particle Size Analysis

Dispersion particle size analyses were made using a Malvern MS 20 particle size analyzer (Malvern Instruments, Malvern, England). Parameters chosen for operation included a lens focal length of 45 mm and an obscuration value maintained in the range 0.14–0.30 (within the instrument ideal range). The background-zeroing liquids used were 95% ethanol and distilled water for shellac and WPI dispersions, respectively. A presentation code of 0409 was used in the measurements, which refers to a refractive index ratio (dispersed phase/continuous phase) of 1.08 and an extinction index (k) of about 0.01. This value for CW and AMF was recommended by scientists at Malvern. The Sauter mean diameter (SMD) was used as the characteristic dimension of the particle size. The SMD is defined as the ratio of the third to second moments of the probability density function of the dispersed particles.[31] It is also called the volume-surface mean, which is the

average size of dispersed particles based on the specific volume per unit surface.[32] The SMD is commonly noted as D[3,2] or d_{32}. Other important parameters include D[v,0.9], D[v,0.5], D[v,0.1], the span, and the shape of the size distribution. D[v,0.9], D[v,0.5], and D[v,0.1] specify the mean particle diameter at the 90th, 50th, and 10th percentiles, respectively.[33] The span gives a measure of the width of the volume distribution relative to the median diameter (D[v,0.5]) and is calculated as (D[v,0.9] − D[v,0.1])/D[v,0.5].

Determination of the Refractive Index of Solid Films

Films used for refractive index measurements were cast on smooth black acrylic plates (TAP Plastics) in the same manner as coatings. Before testing, the films were carefully peeled off the casting surface. HPMC and WPI coatings were transparent and colorless. Shellac coatings had a slight yellow color but were transparent.

The refractive indices of solid WPI, HPMC, and shellac films were determined at 22–24°C using an Abbe refractometer (Milton Roy Co.).[34,35] Contact liquids with high refractive indices (n) used were cedarwood oil (n = 1.5155), methyl iodide (n = 1.5238), and methylene iodide (n 1.7425), all purchased from Sigma Chemical. The refractive index of CW at 23°C ($n \approx 1.4760$) was extrapolated from previously published data.[36,37] The refractive index of AMF at 23°C ($n \approx 1.4545$) was calculated from data given by Parodi and Dunstan.[38] For CW and AMF dispersion coatings, the refractive indices were calculated from the weighted average of refractive indices of the pure CW or AMF and biopolymer components of the coatings. This weighted average method is analogous to that used for the determination of the surface energy of heterogeneous solid surfaces from contact angle measurements.[39]

Gloss Measurements

Gloss was measured using a MICRO-TRI-GLOSS meter (BYK Gardner, Silver Spring, MD). Gloss was measured at the 20°, 60°, and 85° angles from the normal to the coating surface in accordance with American Society for Testing and Materials method D523.[11] Prior to gloss measurements, coatings were conditioned inside acrylic desiccators (catalog number 08-642-23C; Fisher Scientific) for 24 h at 23°C and 75% RH. RH was maintained with saturated sodium chloride solutions.[40] Coatings were removed individually from storage, gloss measured within 30 s, then returned to storage.

In accordance with American Society for Testing and Materials D523, polished black glass, with a refractive index of 1.567, was used as the primary gloss standard.[11] The absorbance coefficient of the standard was assumed to be zero. Gloss values of the matte acrylic casting surfaces were low and measured 0.2, 3, and 10 gloss units (% of standard) for the 20°, 60°, and 85° angles, respectively. These low gloss values ensured that double reflection effects, which interfere with coating gloss measurement, did not occur. Reflectances of biopolymer coatings were calculated from gloss measurements from the definition of G^{θ} values previous described in the Theory section.

Table I Mean Measured Refractive Indices (n) of Biopolymer Coatings at 23°C with Corresponding Sample Size (N) and Standard Error (SE)

Coating	N	n	SE
WPI/GLY, 2 : 1	9	1.5186	0.0020
WPI/GLY, 2 : 1 + 0.36% Span 20	3	1.5173	0.0041
Shellac/PG, 9 : 1	3	1.5222	0.00044
HPMC/GLY, 5 : 1	3	1.4838	0.00024

RESULTS AND DISCUSSION

Refractive Index of Biopolymer Films

The measured refractive indices (n) of transparent edible films had low standard deviations (Table I). Literature values for the refractive index of WPI could not be found. The measured n value for shellac was in good agreement with a previously reported value of 1.5223.[41] The refractive index value for HPMC was similar to that reported for ethyl cellulose (1.479 at 21°C).[42] For calculation of theoretical gloss of transparent coatings, the films were assumed to be nonabsorbing. This is a reasonable assumption for WPI and HPMC, because for an opaque plastic, the k value is about 0.001.[16] Bleached shellac has been shown to be virtually nonabsorbing in the visible wavelength range of 400–700 nm.[43] Reliable refractive index values of zein coatings could not be measured using this refractometer technique. The contact

Table II Model Versus Measured G^{20}, G^{60}, and G^{85} Values of Biopolymer Coatings

	G^{20}		G^{60}		G^{85}	
Coating	Model	Measured	Model	Measured	Model	Measured
WPI/GLY	86.9	72.6	92.2	90.8	99.3	99.1
WPI + Span	88.1	65.6	92.9	87.6	99.4	85.0
Shellac/PG	87.9	76.4	92.8	92.9	99.4	97.2
HPMC/GLY	77.8	29.2	86.4	64.7	98.7	57.2
Zein/PG	85.5	55.4	91.3	91.8	99.2	94.5

liquids used may have had too much interaction with the zein to obtain stable readings.

Comparison of Model and Measured Gloss Values

The measured G^{60} values of transparent WPI (without surfactant) and shellac coatings correlated well with the Fresnel model predictions (Table II). Span 20 addition to WPI coatings slightly decreased measured gloss compared with the model values. WPI coatings with Span 20 also appeared slightly hazier than WPI coatings without surfactant. This may have been attributable to surfactant aggregation at the coating surface during drying, which resulted in WPI coatings with surfactant having lower gloss values than WPI coatings without surfactant (Table II). WPI (with and without Span 20) and shellac coatings were all considered high gloss, because their G^{60} values were ≥ 70.[44] Measured G^{20} values did not correlate as well with predicted values as G^{60} values (Table II). This is partially due to the dependence of reflectance on the angle of incidence and the increased ability of a surface to scatter light at a smaller angle of incidence. Zein coatings also had poor correlation between model and measured G^{20} values. As the angle of incidence of a light beam from the normal of a surface decreases, a smaller cross-sectional area of that beam interacts with the surface. This results in less reflected light. Coating defects and heterogeneity, due to air bubbles, dust particles, polymer-plasticizer phase separation, or other surface irregularities, may have also resulted in lower than expected G^{20} values.

For lipid-containing coatings, model G^{60} values were determined from the calculated refractive indices of WPI-AMF coatings (Fig. 2). It was assumed that the coatings were optically smooth and homogeneous. The WPI-AMF, WPI-CW, and shellac-CW model curves were almost identical to each other. The refractive indices of shellac and WPI were almost the same. CW and AMF also have similar n values. Incorporation of lipids clearly reduced measured gloss as compared with the model predictions (Fig. 2). It is important to note that when the particle size was small (0.31 μm), measured G^{60} values were high. Although these measured G^{60} values were lower than those predicted by the model, increasing lipid did not change measured gloss values. The model and measured G^{60} curves for WPI-AMF coatings were nearly parallel. When particle size was high, the model did not accurately predict gloss. These results indicate that a small particle size promotes a more uniform surface, which is an assumption

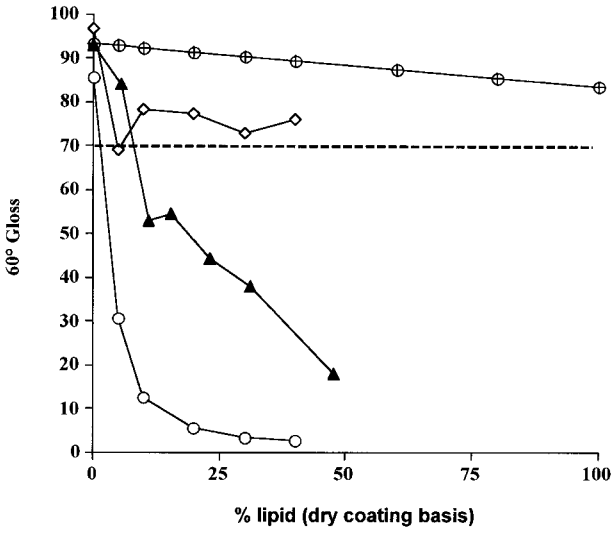

Figure 2 Effect of lipid content on model and measured G^{60} values of WPI and shellac dispersion coatings. (⊕) model; (◇) WPI-AMF measured (SMD = 0.31 μm); (▲) shellac-CW measured (SMD = 1.59 μm); (○) WPI-CW measured (SMD = 1.42 μm). The model curve is calculated using eqs. (5)–(7), assuming optically smooth, homogeneous WPI-AMF surfaces. The dark dashed line shows the cut-off between a high- and low-gloss surface as measured at an angle of 60°.

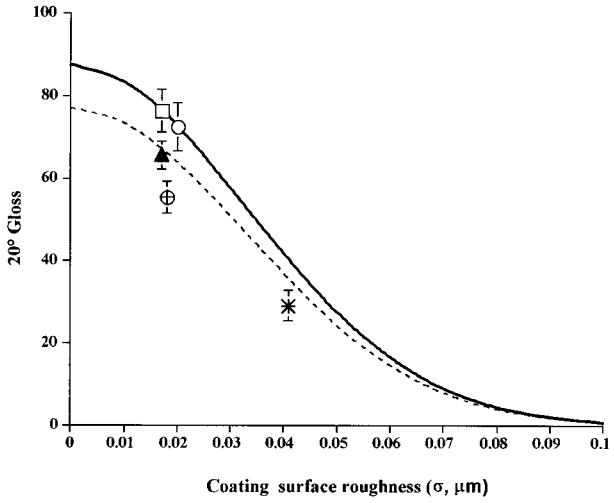

Figure 3 Effect of surface roughness (σ) on the 20° gloss of biopolymer coatings calculated from eq. (9) using incident light at a wavelength of 550 nm. The numbers in parentheses are the coefficients of variation (r^2) values obtained from each linear regression. (—) model using a coating with a refractive index of 1.52; (- -) model using a coating with a refractive index of 1.48; (⊕) measured zein/PG (0.980); (○) measured WPI/GLY (0.962); (□) measured shellac/PG (0.841); (▲) measured WPI/GLY + 0.36% Span 20 (0.991); (*) measured HPMC/PG (0.940). Vertical bars show the standard error about each mean gloss value.

of model calculations. Thus, a small particle size promotes a more homogeneous surface. This is discussed in more detail in the following section.

Surface Roughness and Heterogeneity

Transparent Coatings

The root mean square roughness values (σ) of the transparent biopolymer coatings were low as calculated at a wavelength (λ) of 550 nm (Fig. 3). This λ value is the midway point of the visible range of light, and it is commonly used as a reference wavelength.[9,16,20] Using a similar analysis to that of Simpson,[9] it was found that the roughness of the measured biopolymer coatings fit the model well (Fig. 3). Because gloss is dependent on the refractive index of the surface, model curves for coatings with refractive indices of 1.48 (approximating HPMC coatings) and 1.50 (approximating shellac, zein, and WPI coatings) are included. Zein refractive index was calculated from an estimated n of 1.540 for proteins[-42] and a value of 1.43 for PG.[37] The poor fit of the zein/PG coating to the $n = 1.50$ model suggests that the calculated refractive index (1.513) of the zein/PG coating did not accurately represent the true refractive index of the coating.

The transparent coatings in this study were found to be essentially optically smooth. Using the Raleigh criteria from eq. (10), the maximum σ values that will maintain optical smoothness of coatings are $h < 0.79$, 0.14, and 0.073 μm at 85°, 60°, and 20° angles of measurement, respectively. All coatings had roughness values much less than their Raleigh critical values. As predicted, roughness had no apparent effect on shellac and WPI gloss, as seen from G^{60} values of these coatings greater than 70 (Table II). For HPMC, it is not clear why the measured G^{60} value was 26% lower than the predicted value. It was noticed that HMPC films were slightly tacky after the conditioning period. Because the HPMC coatings were water soluble, sorption of water during storage may have dissolved the polymer, enabling contaminants (such as dust particles) to be incorporated onto the coating surface.

Lipid-Dispersion Coatings

Lipid-dispersion coatings were opaque in appearance, similar to high-density polyethylene milk containers. Lipid content and particle size affected measured G^{60} values (Fig. 2). The lipid portion of WPI-CW, shellac-CW, and WPI-AMF dispersion coatings had SMD values of 1.42, 1.59, and 0.31 μm, respectively. At equal lipid contents, a small SMD clearly favored a high gloss, as all WPI-AMF coatings had G^{60} values $\geq$70 (Fig. 2).

The drop in G^{60} values as a function of lipid content was much steeper for WPI-CW coatings than for shellac-CW coatings. Differences in gloss (at equal lipid levels) are probably not a result of surface roughness. Roughness of WPI-CW and shellac-CW coatings approached σ values of only 0.1 μm (Fig. 4). This value is quite low compared with the particle size of the dispersed phase. Because the CW dispersions had high particle sizes, phase separation during drying most likely occurred. WPI-lipid dispersion films with SMDs greater than 1 μm typically show phase separation during drying.[7] Thus, WPI-CW films in the current study were probably lipid-rich at the air–coating interface. Clusters of lipid particles at the surface would then cause surface heterogeneity. That is, a wide distribution of protein–wax, wax–wax, and wax–air interfaces were created during phase separation. These interfaces scatter more light than a continuous surface, effectively reduc-

ing the gloss of the coating. Increased lipid at the air–coating interface also results in more light being absorbed rather than reflected. Because shellac coatings were cast from ethanol solutions (specific gravity of ≈0.80 at 25°C), some CW particles (specific gravity ≈0.99 at 25°C) settled during drying. The resulting wax-poor air–coating interface should then have a higher gloss than a wax-rich interface. Shellac-wax dispersions are known to settle and they must be mixed thoroughly before use.[45]

Further evidence of a surface heterogeneity effect can be seen by comparing the shapes of the particle size distributions for the three dispersion coatings. WPI-CW particle size distributions were typically flatter and broader than the shellac-CW distributions (Fig. 5). When phase separation did occur, a greater degree of heterogeneity would be formed from the more polydisperse distribution. The WPI-AMF coatings had a small SMD and a narrower particle size distribution than the two CW particle size distributions. Even if phase separation of AMF had occurred during drying, the lipid-rich layer would be more homogeneous than the WPI-CW lipid-rich layer. Most likely, the WPI stabilized the dispersion against phase separation so that the air–coating interface was actually lipid-poor. Thus, during gloss measurements, the light was reflecting mostly from high-gloss WPI surfaces.

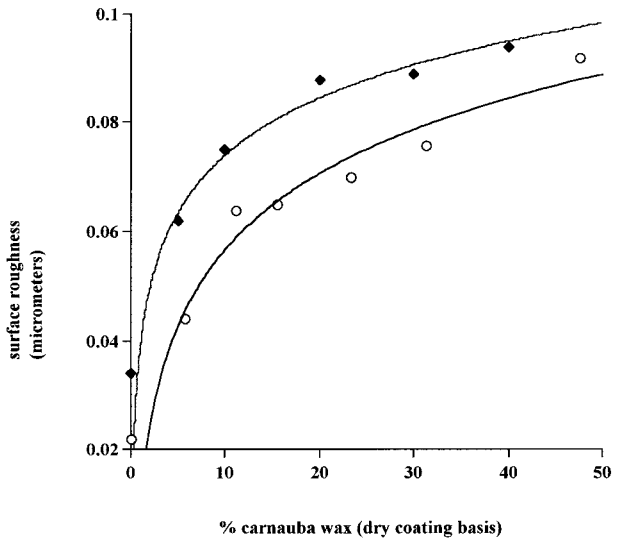

Figure 4 Effect of wax content on the roughness of WPI-CW (♦) and shellac-CW (○) dispersion coatings. SMDs of CW were 1.42 and 1.59 for shellac and WPI dispersions, respectively.

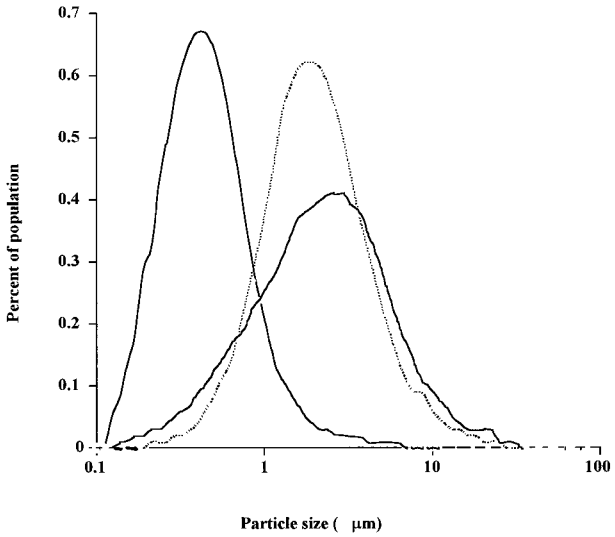

Figure 5 Particle size distributions for the lipid phase of WPI- and shellac-dispersion coatings. (—) WPI-AMF; (· · ·) shellac-CW; (- -) WPI-CW.

CONCLUSIONS

The refractive indices of transparent edible coatings can be used to reasonably predict their gloss properties. The Bennet-Porteus model can be used to estimate the effect of surface roughness on the gloss of biopolymer coatings, provided that accurate values for coating refractive indices are known. The gloss of lipid-dispersion coatings was sensitive to lipid content when the dispersed phase particle size distribution was large and polydisperse. Low SMDs of the dispersed particles and narrow particle size distributions promoted more homogeneous surfaces with high gloss. However, the gloss of heterogeneous surfaces was not accurately predicted from the Fresnel model. Surface heterogeneity had a much larger impact on lipid-dispersion coating gloss than did roughness.

REFERENCES

1. Potter, N. N.; Hotchkiss, J. H. Food Science, 5th ed.; Chapman and Hall: New York, 1995.
2. Musser, J. C. Publication of Speeches and Proceedings of the 27th Annual Production Conference. Pennsylvania Manufacturing Confectioners' Association, Franklin and Marshall College, Lancaster, PA, April 24–26, 1973; PMCA Production Conference Committee: Drexel Hill, PA, 1973.
3. Lecos, C. FDA Consumer. Feb., 1982.

4. Hernandez, E. In Edible Coatings and Films to Improve Food Quality; Krochta, J. M.; Baldwin, E. A.; Nisperos-Carriedo, M., Eds.; Technomic Publishing Co.: Lancaster, PA, 1994; Chapter 10, pp. 279–303.
5. Krochta, J. M. In Food Proteins and Their Applications; Damodaran, S.; Paraf, A., Eds.; Marcel Dekker: New York, 1997; Chapter 18, pp. 529–549.
6. McHugh, T. H.; Krochta, J. M. J Food Process Pres 1994, 18, 173–188.
7. Shellhammer, T. H.; Krochta, J. M. J Food Sci 1997, 62, 390–394.
8. Hagenmaier, R. D.; Baker, R. A. J Food Sci 1996, 61, 562–565.
9. Simpson, L. A. Prog Org Coat 1978, 6, 1–30.
10. Anonymous. Haze-Gloss. Application note; A Color and Appearance Seminar given by BYK-Gardner USA, June 5, 1997, Holiday Inn Select, Foster City, CA; BYK-Gardner USA: Silver Spring, MD.
11. American Society for Testing and Materials. Standard Test Method for Specular Gloss; Designation D 523. 1995 Annual Book of ASTM Standards: Paint-Tests for Chemical, Physical and Optical Properties, Appearance, Durability of Non-Metallic Materials. American Society for Testing and Materials: Philadelphia, 1995; Vol. 6.01.
12. Hunter, R. S.; Harold, R. W. The Measurement of Appearance; John Wiley & Sons: New York, 1987.
13. Rowe, R. C. Pharm Pharmacol 1985, 37, 761–765.
14. Willmouth, F. M. In Optical Properties of Polymers; Meeten, G. H., Ed.; Elsevier Applied Science Publishers: London, 1986; Chapter 5, pp. 265–333.
15. Braun, J. H. J Coating Technol 1991, 63, 43–51.
16. Meeten, G. H. In Optical Properties of Polymers; Meeten, G. H., Ed.; Elsevier Applied Science Publishers: London, 1986; Chapter 1, pp. 1–62.
17. Ward, L. The Optical Constants of Bulk Materials and Films, 2nd ed.; Institute of Physics Publishing: Bristol, England, 1994.
18. Guenther, R. D. Modern Optics; John Wiley & Sons: New York, 1990.
19. Lavin, E. P. Specular Reflection; American Elsevier Publishing: New York, 1971.
20. Tunstall, D. F. J Oil Color Chem Assoc 1967, 50, 989–1007.
21. Mártil, I.; González Díaz, G. Am J Phys 1992, 60, 83–86.
22. Ditchburn, R. W. Light; Academic Press: London, 1976.
23. Born, M.; Wolf, E. Principles of Optics, 5th ed.; Pergamon Press: Oxford, England, 1975.
24. Heavens, O. S. Optical Properties of Thin Solid Films; Dover: New York, 1965.
25. Peiponen, K. E.; Tsuboi, T. Opt Laser Technol 1990, 22, 127–130.
26. Zwinkels, J. C.; Nöel, M. Surf Coat Int 1995, 78, 512–516.
27. Beckman, P.; Spizichino, A. The Scattering of Electromagnetic Waves from Rough Surfaces; Pergamon Press: Oxford, England, 1963.
28. Bennett, H. Industrial Waxes: Natural and Synthetic Waxes; Chemical Publishing: New York, 1975; Vol. 1, p. 170.
29. Johnson, R. E., Jr.; Dettre, R. H. In Surface and Colloid Science; Matijevic, E., Ed.; Wiley-Interscience: New York, 1969; Vol. 2; pp. 86–153.
30. Isganitis, D. K. Manuf Confect 1988, 68, 75–78.
31. Pacek, A. W.; Man, C. C.; Nienow, A. W. Chem Eng Sci 1998, 53, 2005–2011.
32. Stockham, J. D. In Particle Size Analysis; Stockham, J. D.; Fochtman, E. G., Eds.; Ann Arbor Science Publisher: Ann Arbor, MI, 1977; Chapter 1, pp. 1–12.
33. Manual for Mastersizer MS 20; Malvern Instruments: Malvern, England.
34. Pepper, R. E.; Samuels, R. J. In Encyclopedia of Polymer Science and Engineering; John Wiley & Sons: New York, 1985; Vol. 14; pp. 261–298.
35. Lukosz, W.; Pliska, P. Opt Commun 1991, 85, 381–384.
36. Bennett, H. E.; Porteus, J. O. J Opt Soc Am 1961, 51, 123–129.
37. Lide, D. R., Ed. CRC Handbook of Chemistry and Physics, 71st ed.; CRC Press: Boca Raton, FL, 1990; pp. 7–30.
38. Parodi, P. W.; Dunstan, R. J. Aust J Dairy Technol 1971, 26, 29–32.
39. Hiemenz, P. C. Principles of Colloid and Surface Chemistry; Marcel Dekker: New York, 1977.
40. Rockland, L. B. Anal Chem 1960, 32, 1375–1376.
41. Mary Ann Libert, Inc., Publishers. J Am Coll Toxicol 1986, 5, 309–327.
42. Seferis, J. C. In Polymer Handbook, 3rd ed.; Brandrup, J.; Immergut, E. H., Eds.; John Wiley & Sons: New York, 1989; pp. VI-451–461.
43. Goswami, D. N.; Prasad, N.; Das, R.N. J Oil Color Chem Assoc 1981, 64, 20–24.
44. Kible-Boeckler, G. Tappi J 1996, 79, 194–198.
45. Hicks, E. Shellac: Its Origins and Applications; Chemical Publishing: New York, 1961.